REPORT DOCUMENTATION PAGE

Public reporting burden for this collection of information is estimated to average 1 hour per response, including the time for reviewing instructions, searching existing data sources, gathering and maintaining the data needed, and completing and reviewing the collection of information. Send comments regarding this burden estimate or any other aspect of this collection of information, including suggestions for reducing this burden, to Washington Headquarters Services, Directorate for Information Operations and Reports, 1215 Jefferson Davis Highway, Suite 1204, Arlington, VA 22202-4302, and to the Office of Management and Budget, Paperwork Reduction Project (0704-0188), Washington, DC 20503.

1. AGENCY USE ONLY *(Leave blank)*	2. REPORT DATE 18.Jan.01	3. REPORT TYPE AND DATES COVERED MAJOR REPORT

4. TITLE AND SUBTITLE
A PSUEDOLITE CLOSE PROXIMITY STATIC POSITION SOLUTION USING
BIAS KALMAN FILTERING AND PSEUDORANGE SMOOTHING TECHNIQUES

5. FUNDING NUMBERS

6. AUTHOR(S)
2D LT WEYERMULLER SCOTT P

7. PERFORMING ORGANIZATION NAME(S) AND ADDRESS(ES)
UNIVERSITY OF TEXAS AUSTIN

8. PERFORMING ORGANIZATION REPORT NUMBER

CI01-21

9. SPONSORING/MONITORING AGENCY NAME(S) AND ADDRESS(ES)
THE DEPARTMENT OF THE AIR FORCE
AFIT/CIA, BLDG 125
2950 P STREET
WPAFB OH 45433

10. SPONSORING/MONITORING AGENCY REPORT NUMBER

11. SUPPLEMENTARY NOTES

12a. DISTRIBUTION AVAILABILITY STATEMENT
Unlimited distribution
In Accordance With AFI 35-205/AFIT Sup 1

12b. DISTRIBUTION CODE

13. ABSTRACT *(Maximum 200 words)*

14. SUBJECT TERMS

15. NUMBER OF PAGES
41

16. PRICE CODE

17. SECURITY CLASSIFICATION OF REPORT	18. SECURITY CLASSIFICATION OF THIS PAGE	19. SECURITY CLASSIFICATION OF ABSTRACT	20. LIMITATION OF ABSTRACT

A PSEUDOLITE CLOSE PROXIMITY STATIC POSITION SOLUTION

USING BIAS KALMAN FILTERING

AND PSEUDORANGE SMOOTHING TECHNIQUES

by

Scott Paul Weyermuller, M.S.E.

The University of Texas at Austin, 2000

SUPERVISOR: E. Glenn Lightsey

Close proximity space operations require an accurate navigation solution when the line-of-sight to Global Positioning System (GPS) signals becomes blocked. The use of pseudolites in space applications can mitigate this problem. A navigation solution required to pinpoint the location of a static pseudolite receiver in an indoor lab is developed. By using calibration and position Kalman filters to remove code phase biases, unbiased pseudoranges are formed and a position is computed. A more accurate post-processed data solution is also developed from a pseudorange smoothing technique using carrier phases. In simulation, the final smoothed position solution was accurate to the centimeter level, and five-meter accuracy was achieved using lab test data.

20010314 045

A PSEUDOLITE CLOSE PROXIMITY STATIC POSITION SOLUTION

USING BIAS KALMAN FILTERING

AND PSEUDORANGE SMOOTHING TECHNIQUES

by

Scott Paul Weyermuller, M.S.E.

The University of Texas at Austin, 2000

SUPERVISOR: E. Glenn Lightsey

Close proximity space operations require an accurate navigation solution when the line-of-sight to Global Positioning System (GPS) signals becomes blocked. The use of pseudolites in space applications can mitigate this problem. A navigation solution required to pinpoint the location of a static pseudolite receiver in an indoor lab is developed. By using calibration and position Kalman filters to remove code phase biases, unbiased pseudoranges are formed and a position is computed. A more accurate post-processed data solution is also developed from a pseudorange smoothing technique using carrier phases. In simulation, the final smoothed position solution was accurate to the centimeter level, and five-meter accuracy was achieved using lab test data.

References

[1] Lightsey, E. Glenn, "Summer Research Assignment Application: Technology Development for Automated Spacecraft Proximity Flight", Center for Space Research, 1999.

[2] Stone, J.M., et. al., "GPS Pseudolite Transceivers and their Applications", Presented at the ION National Technical Meeting 99, San Diego, California, January 1999.

[3] IntegriNautics IN200C General-Purpose Pseudolite Signal Generator User's Manual, Version 1.0, IntegriNautics Corporation, Palo Alto, California, October 1998.

[4] Zimmerman, K. R., R. H. Cannon Jr., "GPS-Based Control for Space Vehicle Rendezvous", Proceedings of the ASCE Conference on Robotics for Hazardous Environments, Albuquerque, New Mexico, February 1994.

[5] Key, Kevin W., Glenn Lightsey, Robert H. Bishop, "Report of Results on Pseudolite NSTL Study Task From February 1, 1999 – September 30, 1999", Center for Space Research, January 2000.

[6] Mitel Semiconductor GP2000 GPS Architect Receiver Hardware Design Applications Note, Mitel Corporation, Canada, March 1997.

[7] Ndili, Awele, "GPS Pseudolite Signal Design", Presented at ION-GPS-94, Salt Lake City, Utah, September 1994.

[8] Zimmerman, K. R., R. H. Cannon Jr., "Experimental Demonstration of GPS for Rendezvous Between Two Prototype Space Vehicles", Proceedings of the Institute of Navigation GPS-95 Conference, Palm Springs, California, September 1995.

[9] Cobb, Stewart, "Pseudolites and Timetags", E-mail to E. Glenn Lightsey, March 16, 2000.

[10] Hofmann-Wellinhof, B., H. Lichtenegger, J. Collins, Global Positioning System: Theory and Practice, Fourth Edition, Springer, New York, New York, 1997.

[11] Key, Kevin W., "An Introduction to GPS Tracking Loops", Proceedings of the Center for Space Research / University of Texas at Austin Seminar, March 31, 2000.

[12]   Key, Kevin W., "PSD_SIM.EXE, Pseudolite Data Simulator", Center for Space Research, 1999.

[13]   Gelb, Arthur, Applied Optimal Estimation, M.I.T. Press, Massachusetts, 1996.

[14]   Tapley, B. D., B. E. Schutz, G. H. Born, "Excerpts from Statistical Orbit Determination", Center for Space Research / University of Texas at Austin and Colorado Center for Astrodynamics Research / University of Colorado, Academic Press, January 2000.

[15]   Lightsey, E. Glenn, "NSTL1930.00O, NSTL Pseudolite Data", Center for Space Research, July 11, 2000.

References

[1] Lightsey, E. Glenn, "Summer Research Assignment Application: Technology Development for Automated Spacecraft Proximity Flight", Center for Space Research, 1999.

[2] Stone, J.M., et. al., "GPS Pseudolite Transceivers and their Applications", Presented at the ION National Technical Meeting 99, San Diego, California, January 1999.

[3] IntegriNautics IN200C General-Purpose Pseudolite Signal Generator User's Manual, Version 1.0, IntegriNautics Corporation, Palo Alto, California, October 1998.

[4] Zimmerman, K. R., R. H. Cannon Jr., "GPS-Based Control for Space Vehicle Rendezvous", Proceedings of the ASCE Conference on Robotics for Hazardous Environments, Albuquerque, New Mexico, February 1994.

[5] Key, Kevin W., Glenn Lightsey, Robert H. Bishop, "Report of Results on Pseudolite NSTL Study Task From February 1, 1999 – September 30, 1999", Center for Space Research, January 2000.

[6] Mitel Semiconductor GP2000 GPS Architect Receiver Hardware Design Applications Note, Mitel Corporation, Canada, March 1997.

[7] Ndili, Awele, "GPS Pseudolite Signal Design", Presented at ION-GPS-94, Salt Lake City, Utah, September 1994.

[8] Zimmerman, K. R., R. H. Cannon Jr., "Experimental Demonstration of GPS for Rendezvous Between Two Prototype Space Vehicles", Proceedings of the Institute of Navigation GPS-95 Conference, Palm Springs, California, September 1995.

[9] Cobb, Stewart, "Pseudolites and Timetags", E-mail to E. Glenn Lightsey, March 16, 2000.

[10] Hofmann-Wellinhof, B., H. Lichtenegger, J. Collins, Global Positioning System: Theory and Practice, Fourth Edition, Springer, New York, New York, 1997.

[11] Key, Kevin W., "An Introduction to GPS Tracking Loops", Proceedings of the Center for Space Research / University of Texas at Austin Seminar, March 31, 2000.

[12] Key, Kevin W., "PSD_SIM.EXE, Pseudolite Data Simulator", Center for Space Research, 1999.

[13] Gelb, Arthur, <u>Applied Optimal Estimation</u>, M.I.T. Press, Massachusetts, 1996.

[14] Tapley, B. D., B. E. Schutz, G. H. Born, "Excerpts from Statistical Orbit Determination", Center for Space Research / University of Texas at Austin and Colorado Center for Astrodynamics Research / University of Colorado, Academic Press, January 2000.

[15] Lightsey, E. Glenn, "NSTL1930.00O, NSTL Pseudolite Data", Center for Space Research, July 11, 2000.

Vita

Lt Scott Paul Weyermuller was born in Ogden, Utah on February 20, 1977,

the son of Col (Ret) Arthur Paul Weyermuller and Susan Eileen Weyermuller. After

graduating as Valedictorian from Alamogordo High School, Alamogordo, New

Mexico in May 1995, he was awarded an appointment to the United States Air Force

Academy in Colorado Springs, Colorado. A Distinguished Graduate, he received the

degree of Bachelor of Science in Engineering Sciences. He graduated first in his

class in military performance and was commissioned as a Second Lieutenant in the

United States Air Force in June 1999. His first assignment was to earn a Master's

degree in Aerospace Engineering, and in August 1999, he entered The Graduate

School at the University of Texas at Austin.

Permanent Address: 4617 Gonzales Dr.

                            Las Vegas, NV 89130

This report was typed by the author.

Vita

Lt Scott Paul Weyermuller was born in Ogden, Utah on February 20, 1977, the son of Col (Ret) Arthur Paul Weyermuller and Susan Eileen Weyermuller. After graduating as Valedictorian from Alamogordo High School, Alamogordo, New Mexico in May 1995, he was awarded an appointment to the United States Air Force Academy in Colorado Springs, Colorado. A Distinguished Graduate, he received the degree of Bachelor of Science in Engineering Sciences. He graduated first in his class in military performance and was commissioned as a Second Lieutenant in the United States Air Force in June 1999. His first assignment was to earn a Master's degree in Aerospace Engineering, and in August 1999, he entered The Graduate School at the University of Texas at Austin.

Permanent Address: 4617 Gonzales Dr.

                               Las Vegas, NV 89130

This report was typed by the author.

A PSEUDOLITE CLOSE PROXIMITY STATIC POSITION SOLUTION

USING BIAS KALMAN FILTERING

AND PSEUDORANGE SMOOTHING TECHNIQUES

by

Scott Paul Weyermuller, B.S.

Report

Presented to the Faculty of the Graduate School

of the University of Texas at Austin

in Partial Fulfillment

of the Requirements

for the Degree of

Master of Science in Engineering

The University of Texas at Austin

August 2000

A PSEUDOLITE CLOSE PROXIMITY STATIC POSITION SOLUTION

USING BIAS KALMAN FILTERING

AND PSEUDORANGE SMOOTHING TECHNIQUES

APPROVED BY

SUPERVISING COMMITTEE:

_____
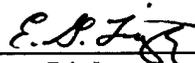
E. Glenn Lightsey

_____
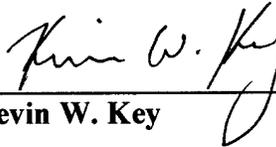
Kevin W. Key

This research is dedicated to my parents and loving fiancée Chauna.

Your support has been unwavering and deeply appreciated.

Date Submitted to Supervising Committee:

11 August 2000

A PSEUDOLITE CLOSE PROXIMITY STATIC POSITION SOLUTION

USING BIAS KALMAN FILTERING

AND PSEUDORANGE SMOOTHING TECHNIQUES

by

Scott Paul Weyermuller, M.S.E.

The University of Texas at Austin, 2000

SUPERVISOR: E. Glenn Lightsey

Close proximity space operations require an accurate navigation solution when the line-of-sight to Global Positioning System (GPS) signals becomes blocked. The use of pseudolites in space applications can mitigate this problem. A navigation solution required to pinpoint the location of a static pseudolite receiver in an indoor lab is developed. By using calibration and position Kalman filters to remove code phase biases, unbiased pseudoranges are formed and a position is computed. A more accurate post-processed data solution is also developed from a pseudorange smoothing technique using carrier phases. In simulation, the final smoothed position solution was accurate to the centimeter level, and five-meter accuracy was achieved using lab test data.

Table of Contents

List of Tables

List of Figures

Chapter 1: Introduction

Since the first surveys were conducted in 1982, numerous GPS applications have been implemented due to its high degree of accuracy. Whether military or civilian in nature, GPS has redefined navigation on Earth as well as in space. It is being used in orbit determination and is beginning to play an important role in spacecraft attitude determination. One of the limitations to GPS, however, is its dependence on line-of-sight signal propagation between the satellite constellation and the receiver. In certain terrestrial applications where an unobstructed view of the sky is not available, pseudolites have been implemented to fill the void.

The National Aeronautics and Space Administration - Johnson Space Center (NASA-JSC), in conjunction with the University of Texas at Austin (UT) Center for Space Research (CSR), is researching the applicability of pseudolites (GPS-like signal propagators) to create a body fixed navigation reference frame for close proximity space vehicle operations [1]. More specifically, the International Space Station (ISS) could benefit from an autonomous navigation system based on GPS signal theory because docking requirements, close proximity formation flight, and Crew Return Vehicle (CRV) flight paths all require accurate navigation. However, these maneuvers could easily lose the required line-of-sight to the GPS constellation when performed close to the large space station. Before a GPS-independent system can be implemented, however, it is important to understand the differences between GPS and pseudolite signals.

This paper first explores the navigation solution required to pinpoint the location of a static pseudolite receiver in an indoor JSC Navigation Systems and Technology Lab (NSTL) using unbiased pseudoranges formed from code phase signals. It then applies a carrier phase smoothing technique to form a more accurate post-processed data solution because the pseudolite signals are propagated extremely close to the receiver in comparison to most GPS applications, and the receiver is subjected to the noisy conditions inherent in the NSTL. The close proximity situation presented in the lab is similar to what will be expected in the ISS reference frame in terms of signal to noise ratios and the unavailability of GPS.

The initial goal of this work was to achieve a static positioning accuracy of five meters (a value slightly larger than predicted code phase accuracy due to lab noise) in simulation. Once this was achieved, the same algorithms were to be applied to pseudolite data taken in the NSTL. The results of this research will be used as a baseline for future relative and kinematic position fixes that can in turn be used to derive relative navigation and collision avoidance algorithms in the ISS reference frame.

Incorporating GPS and pseudolite reception capability into the same receiver could eventually provide a cost effective means to switch from a GPS navigation solution to an autonomous pseudolite navigation system when approaching ISS. Furthermore, such a receiver could help automate close proximity operations and reduce pilot workload. Altogether, a combined GPS and pseudolite navigation system would be a valuable means to separate future ISS traffic.

2

Chapter 2: Pseudolite, Hardware, and Facility Description

Pseudolites are currently used as a means to augment the GPS satellite constellation. They are mainly used when it is desirable to obtain GPS signals in areas where the required lines of sight to the satellites are not readily available or where an increased number of signals is required. Pseudolites are devices that can transmit GPS-like signals, and many current applications include transceiving GPS signals at a fixed location on the Earth's surface into areas with a hindered view of the sky. Such applications include deep pit mining, precision farming, and in future aircraft precision landing systems known as local and wide area augmentation [2].
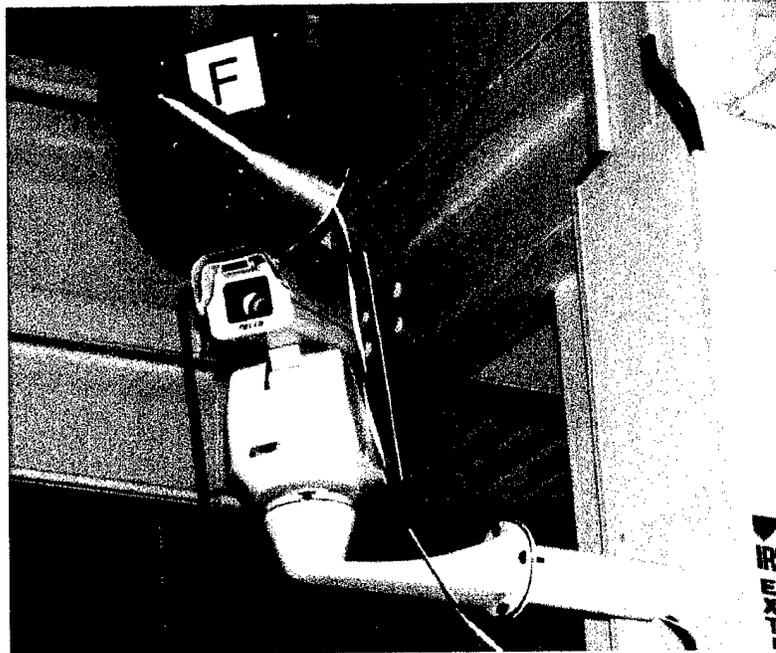
Figure 1: Pseudolite Transceiver Apparatus in NSTL

All of the pseudolite data required for this project was obtained in the NSTL, or high bay lab at JSC. The lab's original configuration had six IntegriNautics

IN200C Pseudolites (Figure 1) positioned so that one was in each of the four top

corners of the lab and two were overhead (Figure 2). Later tests used a four-

pseudolite configuration because two pseudolites were removed for closer study at

CSR. Each pseudolite points toward a reference marker located on a table near the

center of the bay. The marker represents the (0, 0, 0) origin in a lab fixed coordinate

system defined by a theodolite survey. The pseudolites are not moved during or in-

between tests so that their positions in the NSTL remain constant.
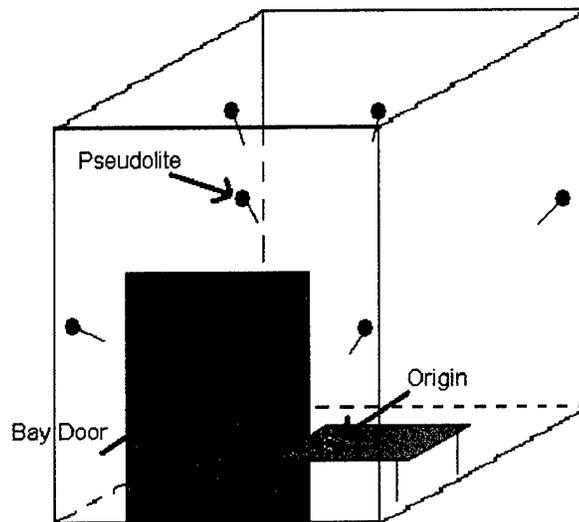
Figure 2: NSTL High Bay Layout (Not to Scale)

The pseudolites used in this research are somewhat simple compared to the

complexities involved with actual GPS satellites. Since their positions are always

fixed, they do not send a navigation data message. Therefore, only *a priori*

knowledge of their locations in the lab coordinate frame is required for data

processing. They only transmit the L1 (1575.42 MHz, 19.0 cm) GPS-like signal

containing code and carrier phase data. Accurate pseudorange data, however, must be manipulated from a code phase, as will be discussed in Chapter 3.

The IN200C pseudolite has programmable power attenuation and an external amplification up to +26 dBm (1 Watt) [3]. This is an important feature because of the high levels of noise inherent in the lab environment. It is important to keep a high signal to noise ratio (SNR) while being careful not to cross correlate the signals as they enter the receiver [4]. All six pseudolites in the lab are referenced to a single oscillator, and the line biases between the oscillator and each pseudolite have been minimized since each of the six lines are approximately the same length [5]. While each pseudolite theoretically ticks at the same transmit time, the true time is unknown to the receiver because a navigation message containing a "GPS time" is not sent.

The receiver used in this research was the Mitel Architect "Ship Channel" receiver. This GPS receiver has programmable capability through software that was modified to track the NSTL pseudolites. Data is retrieved in the Receiver Independent Exchange Format (RINEX) [6]. The software is compiled and uploaded to the receiver, and then RINEX data is downloaded and saved to an external computer. In this application, the data corresponds to the static antenna position over the NSTL lab origin on the workbench (Figure 3). These RINEX files contain pseudorange, carrier phase, Doppler, and code phase data. The code phase data has a 1.023e6 chipping rate that must be manipulated into a pseudorange since the transmitted pseudoranges are inaccurate without correct timing data. The Mitel Architect can accept a navigation data packet, so it is possible for this receiver to

5

receive real GPS data if required. However, new software must be loaded into the

receiver to switch between GPS mode and pseudolite mode.
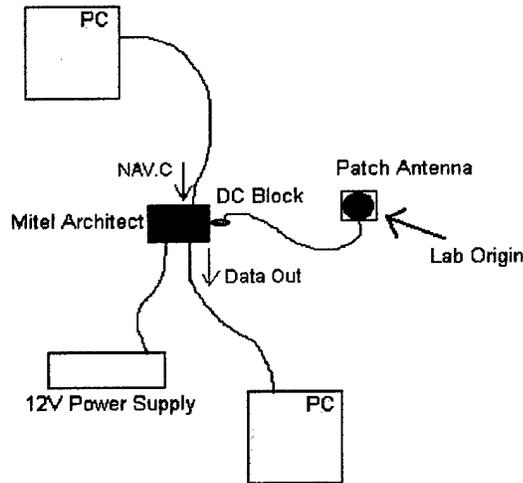
Figure 3: Static Workbench Layout

The tables, equipment, walls and large metal high bay door in the NSTL

produce many opportunities for multipath to occur while taking data. Because the

pseudolites are so close to the receiver (approximately 7 m), there is also the

possibility of the signal not sufficiently spreading before reaching the receiver

antenna, resulting in delayed lock or loss of signals [7] [8]. While difficult to

measure, lab multipath requires careful consideration during data interpretation.

Chapter 3: Pseudoranges from Code Phases

Most of the initial work for this project required a basic understanding of the NSTL setup and operation as well as an understanding of how the Mitel Architect receiver handles pseudolite data. Using data taken previously at the NSTL, a Matlab script was written to read the RINEX observables produced from the Architect. From this script, raw data plots could be formed showing pseudorange, carrier phase, Doppler, and code phase data versus time. The following discussion illustrates how the raw pseudoranges produced by the receiver were inaccurate and how true pseudorange values were calculated from the code phase data.

An initial study of these plots showed that a time tag problem existed because the receiver clock reset itself every 14 seconds. An inquiry to IntegriNautics explained the problem [9]. Although the pseudolites do not transmit relevant navigation data, they transmit navigation packets in the standard ICD-200 format so receivers can still lock onto their signals. Because a pseudolite is not on-orbit like normal GPS satellites and because it does not know the correct GPS time, the navigation message is useless in terms of ephemeris and timing data. The receiver software was written to reject an invalid GPS navigation message, which was causing the software clock to reset. The firmware was modified so the receiver would ignore the contents of the pseudolite data message altogether. This eliminated the resetting time tag problem in future data sets.

Pseudolite	PRN	X Coordinate	Y Coordinate	Z Coordinate	Distance
A	11	-0.0446039	-0.7731419	-6.7365494	6.781
B	8	-0.0303306	3.3911386	-7.0137452	7.791
C	30	-4.1225911	-1.9488081	-3.2345285	5.591
D	20	5.4105458	-2.3215789	-3.3471627	6.773
E	28	2.9573544	5.1741947	-4.1242551	7.248
F	13	-4.2642563	4.4336031	-2.5139543	6.645

Average Distance: 6.805

Table 1: Pseudolite Phase Center Locations (Meters from Lab Origin)

In terms of the NSTL setup, a theodolite survey was taken to accurately

determine the pseudolite phase center coordinates in the lab reference frame prior to

acquiring any relevant data (Table 1). The pseudolites were not moved again after

the survey. Also prior to taking data, the respective power attenuation for each

pseudolite was adjusted to maximize the SNR without getting signal cross correlation

at the receiver. A static position could be computed once the lab coordinate system

was determined, the receiver time tag problem was solved, an algorithm to read the

pseudolite RINEX data had been constructed, and new data had been taken. This

research worked toward a solution exclusively from pseudoranges, so an accurate

position required an accurate pseudorange derivation from the code phase data

present in the data file.

Because the time transmitted is not logged into a navigation message, it has to

be solved using the cycle counts inherent in the code phase data. Investigation of the

firmware code showed that the resolution of the code phase is 2048 samples per chip.

Since one code phase epoch (CDP_{epoch}) has 1023 chips and a rate of 1.023e6 chips per

second, there are 1000 code phase epochs per second:

8

$$\frac{CDP_{epoch}}{1023 Chips} * \frac{1.023e6 Chips}{s} = 1000 \frac{CDP_{epochs}}{s} \qquad (3.1)$$

Introducing the speed of light ($c = 299792458$ m/sec) results in the code phase length of approximately 300km:

$$\frac{c\frac{m}{s}}{1.023e6\frac{Chips}{s}} * \frac{1023 Chips}{CDP_{epoch}} = 299,792\frac{m}{CDP_{epoch}} \qquad (3.2)$$

A pseudorange can be computed as the time-received (Tr) minus the time-transmitted (Tt) in meters, times the speed of light:

$$PR = (Tr - Tt) * c \qquad (3.3)$$

The transmit time is unknown, but it can be computed from code phase since the code phase is sampled at:

$$1023\frac{Chips}{CDP_{epoch}} * 2048\frac{Samples}{Chip} = 2,095,104\frac{Samples}{CDP_{epoch}} = 2,095,104,000\frac{Samples}{s} \qquad (3.4)$$

Hence, pseudoranges can be formed from the speed of light times a quantity containing the fractional part of the received time second minus the code phase measurement (CDP) scaled by the sampling resolution per second and a factor that represents the particular code phase cycle (N):

$$PR = c * (Tr - (\frac{CDP}{2,095,104,000\frac{Samples}{s}} + \frac{N}{1000})) \qquad (3.5)$$

This is the final pseudorange equation computed from code phase measurements. Because of oscillator run-up, the code phase cycle term (N) is a flag

9

that changes the jigsaw scaling effect of the raw code phase data into a continuous

data stream. The post-processed position solution is then formed using Hofmann-

Wellenhof's linear model for point positioning with pseudoranges [10]. The notation

is slightly altered here for consistency and simplicity in single-receiver pseudolite

work, and each term is defined in Table 2:

$$R_j = \rho_j - \frac{X_j - X}{\rho_j} \Delta X - \frac{Y_j - Y}{\rho_j} \Delta Y - \frac{Z_j - Z}{\rho_j} \Delta Z + c\delta_j - c\delta \qquad (3.6)$$

j	Pseudolite number (1-4 in NSTL, 1-6 in simulation)
R_j	Measured code pseudorange from antenna to pseudolite
ρ_j	True geometric distance between antenna and pseudolite
X_j, Y_j, Z_j	NSTL pseudolite coordinates
X, Y, Z	Approximate NSTL antenna coordinates
$\Delta X, \Delta Y, \Delta Z$	Corrections to approximate NSTL antenna coordinates
δ_j	Pseudolite clock offset
δ	Receiver clock offset
c	Speed of light (299792458 m/sec)

Table 2: Pseudorange Point Positioning Linear Model Term Definitions

Four parameters are computed in the state for the least squares position

solution: the location (X, Y, Z) of the receiver antenna with respect to the lab origin

and the clock correction (cdt). An initial guess of $(0, 0, 0, 0)$ is used for the antenna

location and clock offset, and the solution is calculated on an epoch-by-epoch basis.

10

Chapter 4: Code Phase Biases

Initial investigation of the pseudoranges calculated from the code phases showed they were of an order of magnitude equal to that of the speed of light, and code minus carrier plots showed each channel drifting at a different rate. This drift could be explained because the firmware code's original frequency lock loop (FLL) did not directly track carrier phase, but instead tracked their derivatives. A phase lock loop (PLL) was then implemented by Key to directly track the carrier phases, and the resulting code minus carrier plots showed similar drift rates for each channel [11].

The first attempt at calculating a position from code phase determined pseudoranges resulted in (X, Y, Z) coordinates that quickly became undeterminable. The initial $(0, 0, 0, 0)$ position and clock estimate showed the problem became non-linear within a few seconds because of the close proximity (approximately seven meters) of the pseudolites to the receiver in comparison to a large (approximately 300 kilometers) pseudorange measurement. The result was a solution further from the origin at each successive epoch. Trying a new initial estimate using the speed of light to introduce a large order of magnitude in the clock offset state parameter did not have a significant effect on linearizing the solution.

In order to keep the solution from quickly becoming undeterminable, each epoch was then referenced back to the initial guess instead of the previous epoch's solution. These results kept the solution within a more "linear" bound, but large noise

factors still resulted. Again, introducing the speed of light into the initial clock estimate did not alter the solution at all.

The explanation for this result was the evidence of a bias inherent in each pseudolite's code phase. These biases were also determined to be somewhat large. Knowing that each pseudolite was approximately seven meters from the lab origin, it was observed that the code phase computed pseudorange position solution was varying in the fourth order of magnitude because the oscillator to which all of the pseudolites were referenced did not use the fundamental GPS frequency (1.023 MHz) inherent in the receiver. Instead, the reference oscillator used 20.46 MHz. This meant that each pseudolite had the opportunity to begin its code phase data stream at one of twenty different times within the transmit time second. Hence, these biases had to be determined and removed before these pseudoranges could be of any use.

The first attempt at removing the biases was unsuccessful. A second order polynomial was closely fit to a common pseudolite's code phase and was removed from all pseudolites. It was originally thought that the remaining information was the resulting code phase for each respective pseudolite. However, once these code phases were transformed into pseudoranges (discussed in Chapter 3) and later smoothed using carrier phases (later discussed in Chapter 6), the expected white Gaussian noise was not the only error that remained. Consequently, removing a common polynomial from each code phase did not account for the fact that each bias was unique to its corresponding pseudolite. As a result, a Kalman filter approach was implemented to remove each bias before the receiver's position was computed.

12

Chapter 5: Bias Kalman Filter

The overall goal of this work was to achieve a single post processed position solution within five meters of the true position due to the Gaussian white noise on the computed pseudoranges. However, a Kalman filter approach to resolving the code phase biases was chosen as opposed to a batch algorithm so that future work can eventually solve for a real-time solution and eliminate the post-processing requirement. Based on the results presented in Chapter 4, these biases were assumed to resemble a time invariant offset; each one unique and inherent to a pseudolite's code phase. At this point in the research, four pseudolites remained fixed in the NSTL because two of the original six were removed for closer study at CSR. Therefore, it was possible to estimate three of the four biases and dedicate one of the code phases as the reference datum. In other words, one bias was assumed to be zero and the other three were estimated using it as a reference. By including these biases, the pseudorange measurement equation (to each pseudolite j) took the form:

$$PR_j = \rho_j + cdt + \alpha_j + \eta \qquad (5.1)$$

In this equation, the clock offsets from the receiver and reference oscillator were combined into one bias (cdt) common to all four pseudoranges. The first code phase bias (α_1) equaled zero, and there was a unique geometric true range (ρ_j) between the receiver and each pseudolite. The last parameter (η) represented the remaining unknown noise on the measurement that would theoretically carry through to the position solution.

13

Before building a Kalman filter that solved for unknown biases in NSTL data, it was beneficial to filter simulated data first and ensure that known biases could be resolved. Using a pseudolite data simulator (PSD_SIM.EXE) written by Key, pseudorange, carrier phase, smoothed pseudorange, and Doppler data streams subject to the same measurable characteristics observed in the NSTL were created [12]. The simulator returned RINEX data files similar to NSTL tests. The simulated pseudorange (*PR*) information was primarily useful to test the filtering, but the simulated carrier phase (Φ) information was also used to test the smoothing algorithm that will be discussed in Chapter 6. The equations used to produce the simulated data were very similar to those modeled in the NSTL:

$$PR_j = \rho_j + c(dT - dt) + \alpha_j + \eta$$
$$\Phi_j = \rho_j + c(dT - dt) + \lambda N_j + \upsilon$$

(5.2)

This simulator allowed the user to define the output pseudorange and carrier phase noise (η and υ respectively). It also allowed the user to toggle whether the receiver position was offset from the lab origin or in motion, and whether the measurements included line biases (between the reference oscillator and the pseudolites), code and carrier phase biases (α and λN respectively), or reference and receiver clock offset and drift (*dT* and *dt* respectively). The simulated clock offset values were formed from a randomly generated bias and frequency, and the simulated true geometric ranges (ρ) were consistent with those measured in the NSTL theodolite survey. Constant known code phase biases were initially added to "clean"

simulated pseudoranges (with minimal biases and noise), and the Kalman filter resolved those biases perfectly. The simulated biases and noises were then added one at a time to determine how the *a priori* covariance and normal noise distribution matrices should be adjusted as defined in the Kalman filter algorithm below.

Four pseudorange equations were modeled using NSTL data while six equations were modeled using simulated data. There was no significant difference in the filtering by losing two pseudolites. However, estimating the three position parameters (X, Y, Z), the clock offset, and the three code phase biases at one epoch resulted in seven state parameters. A singularity problem occurred because there were four equations and seven unknowns. Adding more pseudolites did not help this problem because each additional pseudolite would add another bias along with its measurement. The singularity occurred while computing the $(HH^T)^{-1}$ portion of the gain matrix. Because a time varying parameter such as motion (velocity or acceleration) was not modeled in this scenario, the observation matrix did not change from epoch to epoch. The HH^T computation was not full rank, and therefore its inverse did not exist when there were more unknowns than equations. Also, each measurement was weighted the same, and the state transition matrix used in the filter did not update any type of dynamics over time. Both of these parameters were therefore modeled as the identity matrix throughout the filtering.

Because of the singularity issue, the final solution to this problem required two Kalman filters. The first was considered a calibration filter used to determine the constant code phase biases and clock offset during a period over a known position.

15

The second filter was used after the calibration period to solve for the receiver's position once the code phase biases were known. In contrast to the receiver clock offset and drift evident in the solution, each code phase bias was different for each pseudolite. Hence for each epoch, the clock bias term was subtracted from each measurement in addition to the unique code phase bias for that pseudolite.

Both filters were derived using the algorithms written by Gelb and Tapley [13] [14]. Constructed using Matlab scripts, the source code for the NSTL data solution can be found in the Appendix. The simulated data position algorithm was only slightly different than the NSTL data algorithm and was therefore not listed here. It only varied in that pseudoranges were not computed from code phases since they were directly provided from the simulated RINEX output file, and the number of measurements was increased from four to six. The entire NSTL data position algorithm is described as follows.

1. Read the raw code phases from RINEX file.

2. Compute the raw (no repeating) pseudoranges (PR's) from the code phases.

3. Initialize the **calibration** nominal sate. Seven meters is the approximate range from the receiver to each pseudolite, cdt represents the entire clock bias (offset and drift), and α represents the respective code phase biases:

$$X_0 = \begin{bmatrix} cdt \\ \alpha_2 \\ \alpha_3 \\ \alpha_4 \end{bmatrix} = \begin{bmatrix} PR_1 - 7 \\ PR_2 - 7 - cdt \\ PR_3 - 7 - cdt \\ PR_4 - 7 - cdt \end{bmatrix} \tag{5.3}$$

16

4. Initialize the **calibration** *a priori* covariance matrix (P_0), normal noise distribution matrix (S), state transition matrix (Φ), and weight matrix (W):

$$P_0 = \begin{bmatrix} 10 & 0 & 0 & 0 \\ 0 & 2 & 0 & 0 \\ 0 & 0 & 2 & 0 \\ 0 & 0 & 0 & 2 \end{bmatrix} \quad S = \begin{bmatrix} 1 & 0 & 0 & 0 \\ 0 & 0.05 & 0 & 0 \\ 0 & 0 & 0.05 & 0 \\ 0 & 0 & 0 & 0.05 \end{bmatrix}$$

$$\Phi = \begin{bmatrix} 1 & 0 & 0 & 0 \\ 0 & 1 & 0 & 0 \\ 0 & 0 & 1 & 0 \\ 0 & 0 & 0 & 1 \end{bmatrix} \quad W = \begin{bmatrix} 1 & 0 & 0 & 0 \\ 0 & 1 & 0 & 0 \\ 0 & 0 & 1 & 0 \\ 0 & 0 & 0 & 1 \end{bmatrix}$$

$$(5.4)$$

5. Loop over all **calibration** epochs of data.

   a. Read epoch.

   b. Propagate the covariance matrix:

   $$P_k = \Phi P_{k-1} \Phi^T + S \tag{5.5}$$

   c. Calculate the observation-state (H) and observation (y) matrices where ρ is the respective (X, Y, Z) norm from the receiver to each pseudolite:

   $$H = \begin{bmatrix} 1 & 0 & 0 & 0 \\ 1 & 1 & 0 & 0 \\ 1 & 0 & 1 & 0 \\ 1 & 0 & 0 & 1 \end{bmatrix} \quad y = \begin{bmatrix} PR_1 - \rho_1 - cdt \\ PR_2 - \rho_2 - cdt \\ PR_3 - \rho_3 - cdt \\ PR_4 - \rho_4 - cdt \end{bmatrix} \tag{5.6}$$

   d. Calculate the gain matrix:

   $$K = P_k H^T \left[H P_k H^T + W^{-1} \right]^{-1} \tag{5.7}$$

   e. Calculate the new estimate:

   $$\hat{x} = Ky \tag{5.8}$$

17

f. Update the state and covariance matrix:

$$X = X + \hat{x} \qquad P_{k-1} = P_k - KHP_k \qquad (5.9)$$

g. Read the next epoch.

6. End the **calibration** loop.

7. Initialize the **position** nominal sate:

$$X_0 = \begin{bmatrix} X \\ Y \\ Z \end{bmatrix} = \begin{bmatrix} 0.0 \\ 0.0 \\ -0.2 \end{bmatrix} \qquad (5.10)$$

8. Initialize the **position** *a priori* covariance matrix (P_0), normal noise

   distribution matrix (S), state transition matrix (Φ), and weight matrix (W):

$$P_0 = \begin{bmatrix} 2 & 0 & 0 \\ 0 & 2 & 0 \\ 0 & 0 & 2 \end{bmatrix} \quad S = \begin{bmatrix} 0.05 & 0 & 0 \\ 0 & 0.05 & 0 \\ 0 & 0 & 0.05 \end{bmatrix}$$

$$\Phi = \begin{bmatrix} 1 & 0 & 0 \\ 0 & 1 & 0 \\ 0 & 0 & 1 \end{bmatrix} \quad W = \begin{bmatrix} 1 & 0 & 0 \\ 0 & 1 & 0 \\ 0 & 0 & 1 \end{bmatrix} \qquad (5.11)$$

9. Loop over all **position** epochs of data.

   a. Read epoch.

   b. Propagate the covariance matrix:

$$P_k = \Phi P_{k-1} \Phi^T + S \qquad (5.12)$$

   c. Calculate the observation-state (H) and observation (y) matrices:

18

$$H = \begin{bmatrix} -\dfrac{X^1 - x}{\rho_1} & -\dfrac{Y^1 - y}{\rho_1} & -\dfrac{Z^1 - z}{\rho_1} \\ -\dfrac{X^2 - x}{\rho_2} & -\dfrac{Y^2 - y}{\rho_2} & -\dfrac{Z^2 - z}{\rho_2} \\ -\dfrac{X^3 - x}{\rho_3} & -\dfrac{Y^3 - y}{\rho_3} & -\dfrac{Z^3 - z}{\rho_3} \\ -\dfrac{X^4 - x}{\rho_4} & -\dfrac{Y^4 - y}{\rho_4} & -\dfrac{Z^4 - z}{\rho_4} \end{bmatrix} \qquad y = \begin{bmatrix} PR_1 - \rho_1 - cdt \\ PR_2 - \rho_2 - cdt - \alpha_2 \\ PR_3 - \rho_3 - cdt - \alpha_3 \\ PR_4 - \rho_4 - cdt - \alpha_4 \end{bmatrix} \qquad (5.13)$$

d. Calculate the gain matrix:

$$K = P_k H^T \left[HP_k H^T + W^{-1} \right]^{-1} \qquad (5.14)$$

e. Calculate the new estimate:

$$\hat{x} = Ky \qquad (5.15)$$

f. Update the state and covariance matrix:

$$X = X + \hat{x} \qquad P_{k-1} = P_k - KHP_k \qquad (5.16)$$

g. Read the next epoch.

10. End the **position** loop.

Using this algorithm to estimate a position solution proved to be very accurate in simulation. Using thirty minutes of simulated data with two meters of noise on the pseudoranges, a random clock offset, random code phase biases, and a receiver location (0.029 m, -0.016 m, −0.172 m) slightly offset form the origin, the following results were obtained. Figure 4 illustrates the calibration clock bias and code phase biases for the six simulated pseudolites.

19
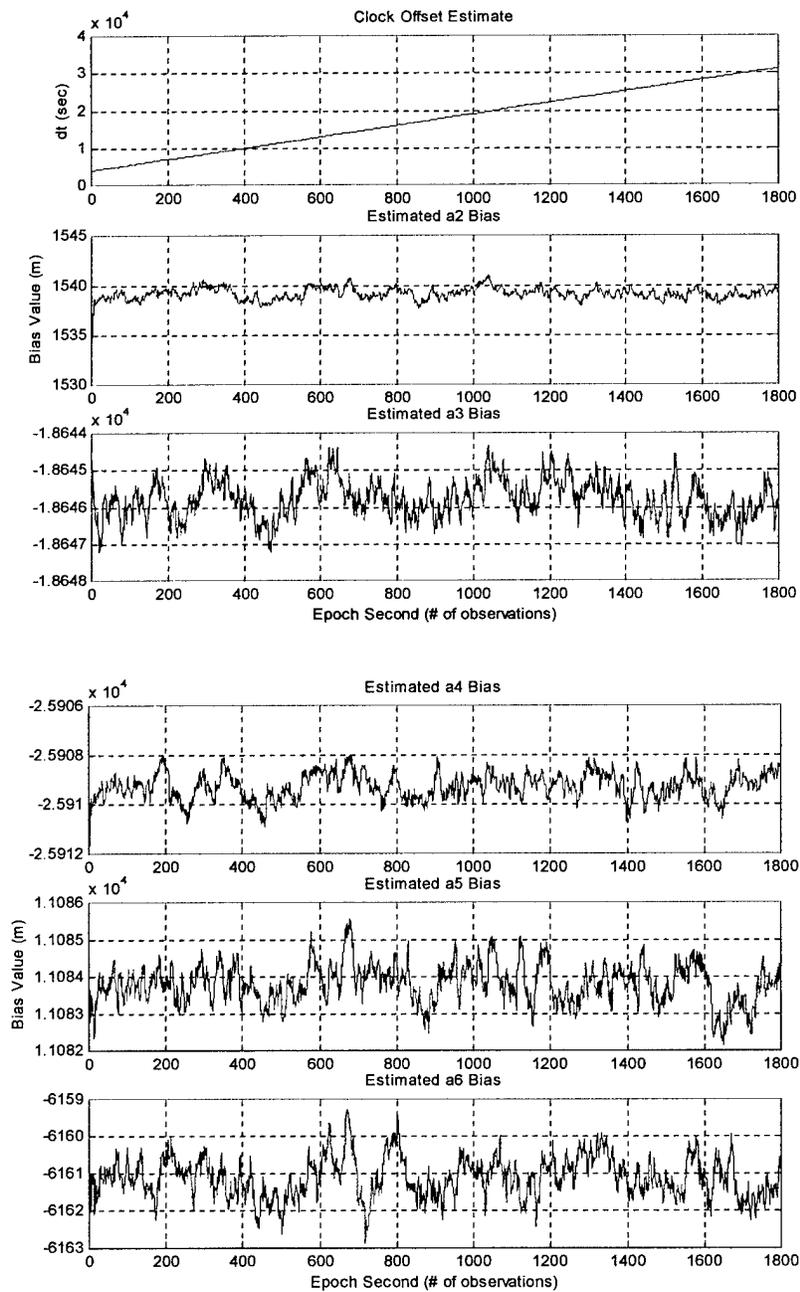
Figure 4: Simulated Clock Bias and Code Phase Biases

The magnitudes of these biases resembled what were expected from NSTL

data. In each case, the filter did not converge to better than two meters of noise on

each bias. It was therefore assumed that the bias value obtained at the end of the filter

was accurate to within the noise inherent in the pseudoranges. Figure 5 illustrates the

simulated position solution estimate after subtracting the biases in Figure 4.
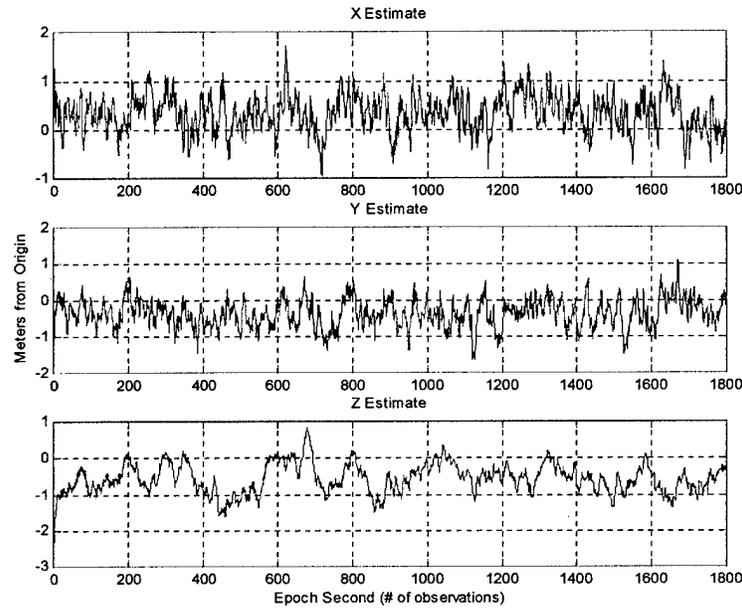
Figure 5: Simulated Position Solution

These results showed approximately two meters of noise and the

characteristics of the original receiver location (0.029 m, -0.016 m, −0.172 m).

Consequently, the calibration-position algorithm was validated for simulated data that

closely resembled what was expected in the NSTL.

Figures 6 and 7 illustrate the unknown biases and position solution estimated

from NSTL data. This data file (NSTL1930.00O) contained an hour of data taken by

Lightsey [15]. The receiver's location was approximately (0.0 m, 0.0 m, −0.2 m).

The negative Z-coordinate described a slight elevation above the origin because the

lab coordinate system was defined using positive values in the "down" direction.
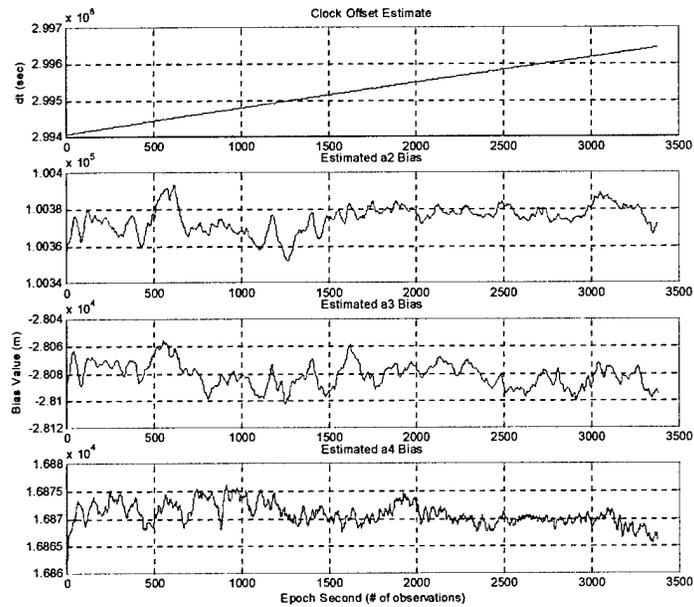
Figure 6: NSTL Clock Bias and Code Phase Biases
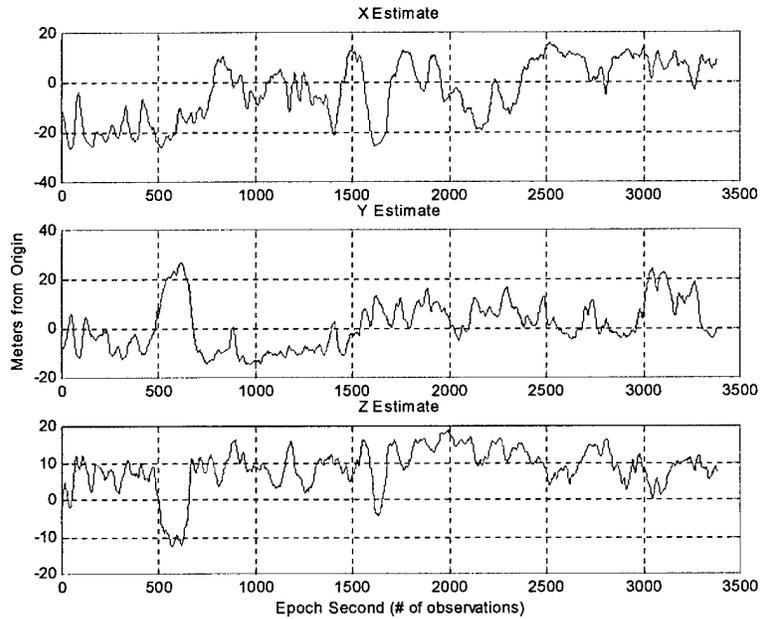
Figure 7: NSTL Position Solution

22

Unfortunately, it was obvious that the NSTL position solution was not nearly as accurate as that formed in simulation. The solution wandered on the order of 30 meters in each direction. Possible reasons for such errors could have been from the assumption that the code phase biases were constant. Studying the code phase bias estimates in the NSTL data (Figure 6) showed a maximum root sum squared (RSS) variation in α_4 of approximately 75 meters around an absolute mean throughout the data file. However, the standard deviations (the square roots of the variances in the covariance matrix) on all four bias estimates (*cdt, α_2, α_3, and α_4*) were approximately 55 centimeters over all of the epochs. This meant that Figure 6 possibly illustrates the true bias at each epoch and not just random noise. Thus, the biases may have been changing over time, or multipath could have been affecting the resulting bias estimates. The error seen in the position solution could have therefore directly transferred from the errors in the bias estimates. Because this solution was not very useful in its current form, a smoothing technique using carrier phases was implemented after the filtering in an attempt to achieve a more precise position.

Chapter 6: Carrier Phase Smoothed Code

Lachapelle's pseudorange smoothing using carrier phases (outlined below from Hoffman-Wellenhof) relies on the increased accuracy provided by the carrier phase data over the noisy pseudoranges [10]. In order to handle the large errors in pseudorange data, the pseudoranges (*PR*) are weighted more heavily during early epochs and the carrier phases (Φ) are weighted more heavily during later epochs. At the first epoch, the weight (*w*) equals one, and it is decreased for each successive epoch by an appropriate factor determined by the length of the data file until the dependence on the pseudoranges is negligible or zero. Although cycle slips have not been found to readily occur in NSTL data files, should one occur, the weight would be reset to one and slowly include the carrier phases again. This smoothed pseudorange equation can be computed as:

$$PR_k sm = wPR_k + (1 - w)(PR_{k-1}sm + \Phi_k - \Phi_{k-1}) \qquad (6.1)$$

For the work done here, full weight was given to the carrier phases after half of the data was processed in order to obtain precision in the position information provided by the pseudoranges. This procedure was coded using a Matlab script in conjunction with a least squares position solution after the pseudoranges were computed from the code phases (described in Chapter 5) and the code phase biases were removed (described in Chapter 6). The NSTL data pseudorange smoothing code can be seen in the Appendix. It should be noted that in kinematic or real-time applications, more weight could be given to the carrier phases at an earlier epoch.

24

Figure 8 shows how this smoothing technique worked very well in simulation. Using the same simulated data file that produced the biases and position estimate in Figures 4 and 5, this technique resulted in centimeter-level error from the actual simulated receiver location (0.029 m, -0.016 m, −0.172 m).
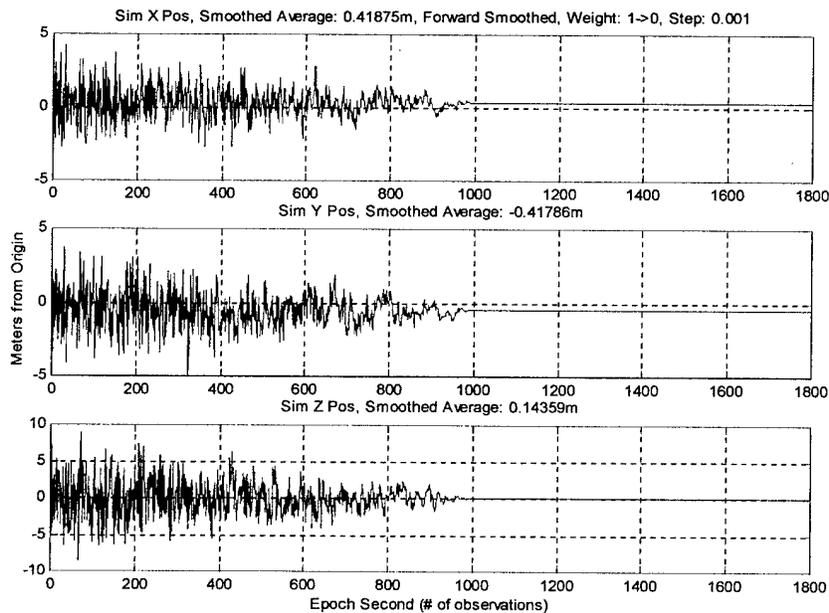
Figure 8: Simulated Smoothed Position Solution

In NSTL data, this smoothing technique also proved to be somewhat useful, but not ideal. Figure 9 shows smoothed pseudoranges from data file NSTL1930.00O after the biases in Figure 6 were removed. The resulting error was approximately five meters from the (0.0 m, 0.0 m, -0.2 m) actual receiver location.
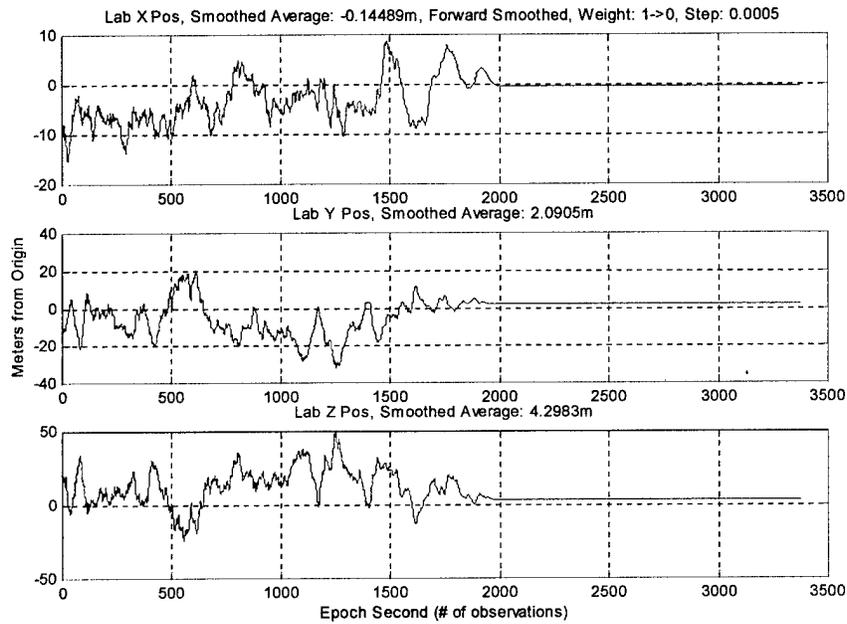
Figure 9: NSTL Smoothed Position Solution

While the NSTL smoothed solution was better than the position estimate

provided by the Kalman filter, it was still not to the expected centimeter-level

accuracy that was achieved in simulation. The combination of filtering and

smoothing the pseudoranges was validated in simulation, but there could still have

been large multipath issues or time-varying code phase biases that caused the NSTL

position estimate to be less accurate.

Chapter 7: Conclusion

Achieving a static position solution from an indoor pseudolite system such as the one studied here in the NSTL is more complicated than normal GPS in certain aspects. Because the code phases were not perfectly synchronized, an extra bias existed in the pseudorange from each pseudolite. A two-step Kalman filter and carrier phase smoothing was required to resolve these biases. The first filter was used during a calibration period over a known location so the constant biases could be determined. The second filter solved for a position once the biases were known.

In simulation, this method worked extremely well. The filter constructed here was successful in determining the biases within a few centimeters in simulated data. The simulated data closely resembled what was expected in real NSTL data because in addition to the code phase biases, it had pseudorange noise and clock biases similar in magnitude to those seen in the NSTL. Although the simulation was designed to model a certain interpretation of the measurement environment, it does not appear to be perfectly consistent with what is observed in the NSTL.

The jump from simulated to NSTL data approximately resulted in a 30-meter increase in bias and position error. Smoothing using the accuracy provided by the carrier phases was then implemented. When both the simulated and NSTL position estimates were smoothed in this manner, the simulated data found the receiver location within a few centimeters while the NSTL solution was accurate to five meters. Table 3 compares the root sum squared (RSS) range of errors in the filtered

position solutions and the root mean squared (RMS) errors in the final smoothed

position solutions from the receiver's true location for both simulated and NSTL data.

		Simulation	NSTL
RSS on	X	2.3	32.0
Calibration/Position	Y	2.2	31.0
Estimate	Z	2.1	32.0
RMS on	X	+ 0.39	- 0.14
Final Smoothed	Y	- 0.40	+ 2.09
Solution	Z	+ 0.32	+ 4.50

Table 3: Position Error Summary (Meters)

While the NSTL position solution from this method was not perfect, it was not

altogether insignificant. The noise and bias characteristics in the lab data were not

perfectly understood, and therefore may not have been perfectly estimated. More

specifically, it could have been possible that the code phase biases were not constant.

They could have varied, as does multipath with time. Multipath itself could have

introduced a large portion of the 30-meter error that forced the position to change

with time because the NSTL was not a controlled environment. Large metal doors

and equipment, the operation of nearby electronic equipment, and people's

movements within the lab could have all magnified the effects of multipath while the

tests were conducted.

Moreover, the hardware or the post-processing algorithm may have been

inaccurate. If the pseudolites and the oscillator were not exactly synchronized in the

manner described in Chapters 2 and 3, time varying biases may have been produced

by the hardware. Otherwise, the understanding of the firmware code that resulted in

the code phase to pseudorange derivation in Chapter 3 may have been incorrect.

Depending on the magnitude of the problem, erroneous pseudoranges could have resulted in additional, possibly time-varying, biases that were not properly modeled in the filtering.

In any event, it is recommended that the next step is to validate the variability in the code phase biases. As an example, motion could be applied to the receiver after the calibration period to determine if that motion can be modeled using the constant biases resolved by this filter. If the five-meter noise is still apparent on the smoothed solution but the motion can be deciphered, then the noisy results seen here may very well be the best available solution under the NSTL environment.

If a motion test does not isolate the situation as a time-varying bias problem, then the answer may be that the code phases must be properly synchronized in order to get a static position solution using only the pseudoranges. In reality, this would be a significant recommendation to negate the errors inherent in the filtering.

Regardless, the work accomplished here did achieve a five-meter solution in an extremely noisy environment. In space, an entirely different environment will be encountered, and new problems will most likely appear. Nonetheless, this work has provided valuable insight into pseudolites and is a stepping-stone to eventual kinematic pseudolite applications in space.

Appendix

```
%Scott Weyermuller
%Code Phase Bias Kalman Filter During Calibration Period
%Open observation file using startpseud.m and readcdp.m to read PR's
%prior to running this script
%Last Updated 3 Aug 2000
%*********************************************************************

clear X_0 X xhat Pbar Pkmin1 Pk P S H y Phi W K
clear outH outy outK outxhat outX outP Obs beg obstime


%Set constants
c=299792458.0;              %speed of light in m/s
pseud=size(sv,2);           %pseud is # of observed pseudolites (4)
obstime=size(time,1);       %obstime is # of observation times (3379)


%Read NSTL pseudolite coordinates
plab193;


%Initialize all matrix dimensions
X_0=zeros(4,1);             %Initial guess of state values
X=zeros(4,1);               %New state after each epoch
xhat=zeros(4,1);            %State update after each epoch
Pbar=zeros(4,4);            %Apriori covariance matrix
Pkmin1=zeros(4,4);          %Covariance matrix of last epoch
Pk=zeros(4,4);              %Covariance matrix of current epoch
P=zeros(4,4);               %Covariance matrix holder
S=zeros(4,4);               %Normal noise distribution matrix
H=zeros(4,4);               %Model matrix
y=zeros(4,1);               %Observed-Computed equation
K=zeros(4,4);               %Gain matrix


%Set initial value of nominal X (dti, a2i, a3i, a4i)
dti=PR(1,1)-7;
a2i=PR(1,2)-7-dti;
a3i=PR(1,3)-7-dti;
a4i=PR(1,4)-7-dti;
X_0=[dti, a2i, a3i, a4i];


%Fill apriori covariance matrix
Pbar(1,1)=10;
```

```
Pbar(2,2)=2;
Pbar(3,3)=2;
Pbar(4,4)=2;
Pkmin1=Pbar;          %Last epoch covariance equals apriori for first computation

%Fill S matrix to open noise search parameters in covariance matrix
S(1,1)=1;
S(2,2)=.05;
S(3,3)=.05;
S(4,4)=.05;

%Fill estimate, state transition and weight matrices
X(1:4)=X_0;           %First epoch uses initial guess of state
Phi=eye(4);           %State transition matrix equals identity
W=eye(4);             %Weight matrix equals identity

calpos=[0.0 0.0 -0.2];

%Loop over all observation times
for oloop=1:obstime

    %Propogate covariance matrix to current epoch
        Pk=Phi*Pkmin1*Phi'+S;

    %Begin available pseudolite loop
    for ploop=1:pseud

        %Calculate range from last receiver position (estimate)
        posdiff=pl(ploop,1:3)-calpos;
        range=norm(posdiff);

        %Fill H matrix with clock offset and bias values
        H(ploop,1)=1;     %Use 1 here instead of c to avoid singularity issues later
        H(2,2)=1;
        H(3,3)=1;
        H(4,4)=1;

        %Fill y vector (observed-computed) for all pseudorange values
        if ploop==1       %First PR bias equals zero, so don't include here
            y(ploop)=PR(oloop,ploop)-range-X(1);
        else
            y(ploop)=PR(oloop,ploop)-range-X(1)-X(ploop);
        end
```

```
%End available pseudolite loop
end

%Calculate gain matrix
K=Pk*H'*inv(H*Pk*H'+inv(W));

%Calculate new estimate and update estimated state
xhat=K*y;
X=X+xhat;

%Update covariance matrix
P=Pk-K*H*Pk;
Pkmin1=P;

%Store output values
outH(:,:,oloop)=H;
outy(:,:,oloop)=y;
outK(:,:,oloop)=K;
outxhat(:,:,oloop)=xhat;
outX(:,:,oloop)=X;
outP(:,:,oloop)=P;
Obs(oloop)=oloop;

%End observation time loop
end

%Manipulate stored output values for plots
update=squeeze(outxhat);          %Holds bias updates for each epoch
uClkrec=update(1,:);
ua2=update(2,:);
ua3=update(3,:);
ua4=update(4,:);


posn=squeeze(outX);               %Holds updated state for each epoch
Clkrec=posn(1,:);
a2=posn(2,:);
a3=posn(3,:);
a4=posn(4,:);
Xfinal=X;

%Plot results
```

32

```
%Scott Weyermuller
%X,Y,Z Position Kalman Filter After Calibration Period
%Open observation file using startpseud.m, form PR's using readcdp.m, and find
%code phase biases using kalmanbias.m prior to running this script
%Last Updated 3 Aug 2000
%*******************************************************************

clkrem=outX;

clear X_0 X xhat Pbar Pkmin1 Pk P S H y Phi W K outH outy outK outxhat outX
outP Obs beg obstime posdiff range

C1rem(:,1)=PR(:,1);
C1rem(:,2)=PR(:,2)-Xfinal(2);
C1rem(:,3)=PR(:,3)-Xfinal(3);
C1rem(:,4)=PR(:,4)-Xfinal(4);

%Set constants
c=299792458.0;                  %speed of light in m/s
pseud=size(sv,2);               %pseud is # of observed pseudolites (4)
obstime=size(time,1);           %obstime is # of observation times (3379)

%Read NSTL pseudolite coordinates
plab193;

%Initialize all matrix dimensions
X_0=zeros(3,1);                 %Initial guess of state values
X=zeros(3,1);                   %New state after each epoch
xhat=zeros(3,1);               %State update after each epoch
Pbar=zeros(3,3);               %Apriori covariance matrix
Pkmin1=zeros(3,3);             %Covariance matrix of last epoch
Pk=zeros(3,3);                 %Covariance matrix of current epoch
P=zeros(3,3);                  %Covariance matrix holder
S=zeros(3,3);                  %Normal noise distribution matrix
H=zeros(4,3);                  %Model matrix
y=zeros(4,1);                  %Observed-Computed equation
K=zeros(3,4);                  %Gain matrix

%Set initial value of nominal X (xi, yi, zi)
xi=0.0;
yi=0.0;
zi=-0.2;
X_0=[xi, yi, zi];
```

33

```
%Fill apriori covariance matrix
Pbar(1,1)=2;
Pbar(2,2)=2;
Pbar(3,3)=2;
Pkmin1=Pbar;           %Last epoch covariance equals apriori for first computation

%Fill S matrix to open noise search parameters in covariance matrix
S(1,1)=.05;
S(2,2)=.05;
S(3,3)=.05;

%Fill estimate, state transition and weight matrices
X(1:3)=X_0;            %First epoch uses initial guess of state
Phi=eye(3);           %State transition matrix equals identity
W=eye(4);             %Weight matrix equals identity

%Loop over all observation times
for oloop=1:obstime

  %Propogate covariance matrix to current epoch
        Pk=Phi*Pkmin1*Phi'+S;

  %Begin available pseudolite loop
  for ploop=1:pseud

    %Calculate range from last receiver position (estimate)
    posdiff=pl(ploop,1:3)-X(1:3)';
    range=norm(posdiff);

    %Fill H matrix with range values
    H(ploop,1)=-(pl(ploop,1)-X(1))/range;
    H(ploop,2)=-(pl(ploop,2)-X(2))/range;
    H(ploop,3)=-(pl(ploop,3)-X(3))/range;

    %Fill y vector (observed-computed) for all pseudorange values
    y(ploop)=C1rem(oloop,ploop)-range-clkrem(1,1,oloop);

  %End available pseudolite loop
  end

%Calculate gain matrix
K=Pk*H'*inv(H*Pk*H'+inv(W));
```

```
%Calculate new estimate and update estimated state
xhat=K*y;
X=X+xhat;

%Update covariance matrix
P=Pk-K*H*Pk;
Pkmin1=P;

%Store output values
outH(:,:,oloop)=H;
outy(:,:,oloop)=y;
outK(:,:,oloop)=K;
outxhat(:,:,oloop)=xhat;
outX(:,:,oloop)=X;
outP(:,:,oloop)=P;
Obs(oloop)=oloop;

%End observation time loop
end

%Manipulate stored output values for plots
update=squeeze(outxhat);              %Holds updates for each epoch
uposx=update(1,:);
uposy=update(2,:);
uposz=update(3,:);

posn=squeeze(outX);                   %Holds updated state for each epoch
posx=posn(1,:);
posy=posn(2,:);
posz=posn(3,:);
Xfinalpos=X;

%Plot results
```

```
%Scott Weyermuller
%GPS Pseudolite Point Positioning Algorithm Using Lab Carrier-Smoothed PR's
%Run startpseud.m and readcdp.m prior to running this script to read PR's
%Specify which plab.m PL coordinates to use and which type of position
%(C1, PR, smPR, C1sm, etc.) to calculate
%Last Updated 3 Aug 2000
%***********************************************************************

clear A l Q dx;

file='nstl1931.00o';
c=299792458.0;                  %speed of light in m/s
n=size(sv,2);                   %n is # of observed pseudolites (4)
m=size(time,1);                 %m is # of observation times (3379)
w = 1;
wvar = 0.0005;
wmin = 0.0;


global file m n

%Call smoothing function and read PL lab coordinates
[C1sm, avg] = smooth(C1rem, L1, w, wvar, wmin);
plab193;

%Initial receiver position and clock guess
pos0=[xi, yi, zi, dti];

  %Begin observation time loop
  for iloop=1:m

   %Begin available sat loop
   for j=1:n

        %Calculate range from last receiver position
        pos0diff=pl(j,1:3)-pos0(1:3);
        range=norm(pos0diff);

        %Fill A matrix for all sat's (let c=1)
        A(j,1)=-(pl(j,1)-pos0(1))/range;
        A(j,2)=-(pl(j,2)-pos0(2))/range;
        A(j,3)=-(pl(j,3)-pos0(3))/range;
        A(j,4)=1;
```

36

```
                %Fill l vector for all pl's when bias is estimated
                l(j)=C1sm(iloop,j)-range-clkrem(1,1,iloop);

        %End available sat loop
                end

        %Fill cofactor matrix
        Q=inv(A'*A);

        %Compute gdop and dx
        gdop=sqrt(Q(1,1)+Q(2,2)+Q(3,3)+Q(4,4));
        dx=Q*A'*l';

        %Update receiver position for successive iterations
        pos(1)=pos0(1)+dx(1);
        pos(2)=pos0(2)+dx(2);
        pos(3)=pos0(3)+dx(3);
        pos(4)=pos0(4)+dx(4);

        %Store values for plots
        Posx(iloop)=pos(1);
        Posy(iloop)=pos(2);
        Posz(iloop)=pos(3);
        Clkrec(iloop)=pos(4);
        GDOP(iloop)=gdop;
        DOPx(iloop)=Q(1,1);
        DOPy(iloop)=Q(2,2);
        DOPz(iloop)=Q(3,3);
        DOPt(iloop)=Q(4,4);
        Obs(iloop)=iloop;

%End observation time loop
end

mx=num2str(mean(Posx(avg:m)));
my=num2str(mean(Posy(avg:m)));
mz=num2str(mean(Posz(avg:m)));
w=num2str(w);
wmin=num2str(wmin);
wvar=num2str(wvar);

%Plot values vs # of observations
```

```
%Scott Weyermuller
%PR Smoothing Function from Carrier Phases
%Run startpseud.m and readcdp.m prior to running this script to read PR's
%Specify which plab.m PL coordinates to use and which type of position
%(C1, PR, smPR, C1sm, etc.) to calculate
%Last Updated 3 Aug 2000
%*********************************************************************

function [C1sm, avg] = smooth(PR, L1, w, wvar, wmin);

global file m n

start = 1;
stop = size(PR,1);
c = 299792458.0;               %speed of light in m/s
f1 = 1575.42e6;                %L1 frequency in MHz
L1_m = L1 * c / f1;            % carrier phase in meters

C1sm = PR;
once = 1;

%Begin observation time loop
for t = 2:m

  C1sm(t,:) = w*PR(t,:)+(1-w)*(C1sm(t-1,:)+L1_m(t,:)-L1_m(t-1,:));

  w = w-wvar;
  if w < wmin
    if once==1
      avg = t
      once=2;
    end
    w = wmin;
  end

end
```

References

[1]   Lightsey, E. Glenn, "Summer Research Assignment Application: Technology Development for Automated Spacecraft Proximity Flight", Center for Space Research, 1999.

[2]   Stone, J.M., et. al., "GPS Pseudolite Transceivers and their Applications", Presented at the ION National Technical Meeting 99, San Diego, California, January 1999.

[3]   IntegriNautics IN200C General-Purpose Pseudolite Signal Generator User's Manual, Version 1.0, IntegriNautics Corporation, Palo Alto, California, October 1998.

[4]   Zimmerman, K. R., R. H. Cannon Jr., "GPS-Based Control for Space Vehicle Rendezvous", Proceedings of the ASCE Conference on Robotics for Hazardous Environments, Albuquerque, New Mexico, February 1994.

[5]   Key, Kevin W., Glenn Lightsey, Robert H. Bishop, "Report of Results on Pseudolite NSTL Study Task From February 1, 1999 – September 30, 1999", Center for Space Research, January 2000.

[6]   Mitel Semiconductor GP2000 GPS Architect Receiver Hardware Design Applications Note, Mitel Corporation, Canada, March 1997.

[7]   Ndili, Awele, "GPS Pseudolite Signal Design", Presented at ION-GPS-94, Salt Lake City, Utah, September 1994.

[8]   Zimmerman, K. R., R. H. Cannon Jr., "Experimental Demonstration of GPS for Rendezvous Between Two Prototype Space Vehicles", Proceedings of the Institute of Navigation GPS-95 Conference, Palm Springs, California, September 1995.

[9]   Cobb, Stewart, "Pseudolites and Timetags", E-mail to E. Glenn Lightsey, March 16, 2000.

[10]   Hofmann-Wellinhof, B., H. Lichtenegger, J. Collins, Global Positioning System: Theory and Practice, Fourth Edition, Springer, New York, New York, 1997.

[11]   Key, Kevin W., "An Introduction to GPS Tracking Loops", Proceedings of the Center for Space Research / University of Texas at Austin Seminar, March 31, 2000.

[12]   Key, Kevin W., "PSD_SIM.EXE, Pseudolite Data Simulator", Center for Space Research, 1999.

[13]   Gelb, Arthur, <u>Applied Optimal Estimation</u>, M.I.T. Press, Massachusetts, 1996.

[14]   Tapley, B. D., B. E. Schutz, G. H. Born, "Excerpts from Statistical Orbit Determination", Center for Space Research / University of Texas at Austin and Colorado Center for Astrodynamics Research / University of Colorado, Academic Press, January 2000.

[15]   Lightsey, E. Glenn, "NSTL1930.00O, NSTL Pseudolite Data", Center for Space Research, July 11, 2000.

Vita

Lt Scott Paul Weyermuller was born in Ogden, Utah on February 20, 1977,

the son of Col (Ret) Arthur Paul Weyermuller and Susan Eileen Weyermuller. After

graduating as Valedictorian from Alamogordo High School, Alamogordo, New

Mexico in May 1995, he was awarded an appointment to the United States Air Force

Academy in Colorado Springs, Colorado. A Distinguished Graduate, he received the

degree of Bachelor of Science in Engineering Sciences. He graduated first in his

class in military performance and was commissioned as a Second Lieutenant in the

United States Air Force in June 1999. His first assignment was to earn a Master's

degree in Aerospace Engineering, and in August 1999, he entered The Graduate

School at the University of Texas at Austin.

Permanent Address: 4617 Gonzales Dr.

                          Las Vegas, NV 89130

This report was typed by the author.